# How Does the Deep Western Boundary Current Cross the Gulf Stream?*

ROBERT S. PICKART

*Woods Hole Oceanographic Institution, Woods Hole, Massachusetts*

WILLIAM M. SMETHIE, JR.

*Lamont-Doherty Geological Observatory, Columbia University, Palisades, New York*

(Manuscript received 18 June 1992, in final form 9 February 1993)

ABSTRACT

The manner in which the deep western boundary current (DWBC) crosses the Gulf Stream is investigated using data from a hydrographic survey conducted in 1990. Absolute geostrophic velocity vectors are computed using in situ float data to obtain the reference level. Three density layers are considered in detail: two mid-depth layers, which together make up the shallowest water mass component of the DWBC (500–1200 m), and a deep layer consisting of the Norwegian–Greenland overflow water (2500–3500 m). The shallowest layer does not make it through the crossover and is completely entrained by the Gulf Stream; however, the resulting drop in equatorward transport is almost completely replenished by offshore entrainment just south of the crossover. In the intermediate layer, which is denser than the Gulf Stream coming off the shelf, part of the DWBC recirculates to the northeast while the onshoremost portion continues equatorward. In the deep layer only a small amount of recirculation occurs. The lateral fields of potential vorticity ($Q$) reveal a $Q$ barrier associated with the Gulf Stream in the two mid-depth layers, which is partially lessened in the intermediate one allowing the equatorward continuation of flow. In the deep layer, the DWBC maintains its potential vorticity through the crossover.

## 1. Introduction

As the Gulf Stream flows off the continental shelf into deep water it crosses the equatorward flowing deep western boundary current (DWBC). Recent evidence suggests that the DWBC may in fact dynamically influence the separation of the Gulf Stream. A variety of numerical experiments (e.g., Thompson and Schmitz 1989) have shown that the separation latitude of the Gulf Stream is sensitive to the transport of the DWBC (larger transport implies a more southerly separation). The converse problem has also been studied, that is, how the crossover effects the DWBC. Hogg and Stommel (1985) showed that in order to maintain a constant layer thickness the DWBC should flow into deeper water upon crossing under the Gulf Stream.

In the above work, the problem has been addressed from a two-layer standpoint: the Gulf Stream is confined to the upper layer and the DWBC to the lower layer (i.e., a true "crossover"). From a deployment of deep floats, Barrett (1965) concluded that the DWBC flows under the Gulf Stream with apparently no consequence. Using short-term bottom current meter records and a corresponding hydrographic section, Richardson (1977) concluded the same. These results may have helped motivate the separate-layer modeling approach. Recently, Agra and Nof (1993) considered the collision of two opposing boundary currents (with the same density or different densities) that separate from the boundary and flow into the interior as a single current. They found that substantial separation can occur even with large differences in the flow speed of the opposing currents.

In fact, the DWBC is not confined to the abyssal layer. West of the Grand Banks it comprises three separate water masses, which together span the water column from roughly 700 m to the bottom [see Pickart (1992a) for a review]. The two deeper components, the Norwegian–Greenland overflow water and Labrador Sea Water, are able to cross underneath the Gulf Stream. However, it is not at all clear how the shallowest component can negotiate its way past the Gulf Stream, which has significant subsurface transport at this depth. The shallow DWBC (which may be more accurately termed a mid-depth current) originates south of the Labrador Sea (see Pickart 1992a). Its unique distinguishing feature downstream is a strong chlorofluorocarbon (CFC) core. The present study contains the first unambiguous velocity sections of this flow, which give a surprisingly large (synoptic) transport of 12–13 Sv (Sv $\equiv 10^6$ m$^3$ s$^{-1}$). At least some of this water progresses past the Gulf Stream since the CFC core is found against the western boundary at southern latitudes (e.g., Fine and Molinari 1988).

* WHOI Contribution Number 8040.

*Corresponding author address:* Dr. Robert S. Pickart, Woods Hole Oceanographic Institution, Woods Hole, MA 02543.

This paper presents results from a hydrographic survey designed to investigate the crossing of the Gulf Stream and DWBC. Our goal is to gain a better understanding of the kinematics and dynamics of the crossover and to motivate further study of the basin-wide consequences. Special focus is placed on the upper crossing to resolve the apparent contradiction noted above. It is found that throughout the water column both the DWBC and Gulf Stream are significantly altered as they cross. The upper layer will be considered first, then the deep layer containing the Norwegian–Greenland overflow water.

## 2. The hydrographic program

In summer 1990 a 17-day hydrographic survey of the crossover was completed consisting of five finely resolved sections: two upstream (in the DWBC sense) of the crossover, one precisely at the crossover, and two downstream (Fig. 1). In addition to dissolved oxygen and nutrients, CFCs were measured to identify the upper DWBC water mass. The central section coincided with a line of bottom current meters and inverted echo sounders maintained as part of the three-year Synoptic Ocean Prediction (SYNOP) Experiment (see Pickart and Watts 1990). These additional data proved most useful. At each station an acoustic transport float (or POGO float, see Rossby et al. 1991) was deployed to obtain a direct measurement of the vertically integrated velocity to some predetermined depth (usually 1000 m).

### *Absolute geostrophic velocities*

The purpose of collecting the float data was to reference the geostrophic velocities. Of course, since the POGO velocity is a direct measurement, it contains all ageostrophic contributions that were present during the float's deployment. This includes Ekman effects, internal waves, and ageostrophy due to the Gulf Stream jet. However, Pickart and Lindstrom (1993) demonstrate that all three of these effects should have minimal impact on the POGO measurement. The POGO float extends deep enough to effectively reduce (by averaging

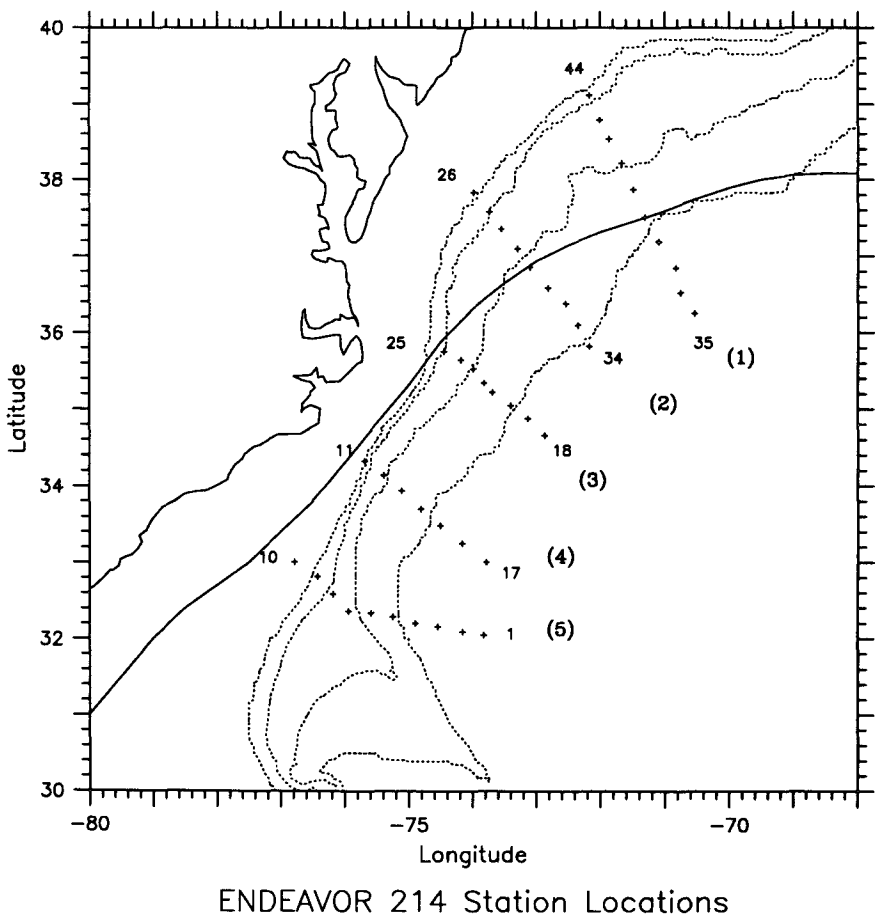


FIG. 1. Station locations of Endeavor 214; section numbers are in parentheses. The solid line is the mean location of the Gulf Stream north wall (P. Cornillon, personal communication; Olson et al. 1983).

out) the internal wave signal, while the Ekman contribution is small due to its minimal vertical extent and amplitude. Regarding the Gulf Stream signal, the largest source of ageostrophy that Johns et al. (1989) found at 73°W (near our section 2) was a gradient wind effect due to the strong curvature of the Gulf Stream. This was confined to the upper layer, and thus should have minimal impact on a deep-reaching POGO, which spends most of its time in the subsurface geostrophic Gulf Stream. Furthermore, during the time of our hydrographic survey the curvature of the Gulf Stream was nearly zero (Pickart and Lindstrom 1993). One source of ageostrophy that will affect the POGO is the barotropic tide, but this is generally small in deep water; Pickart and Lindstrom (1993) calculated the amplitude of the barotropic tide at section 3 using the SYNOP current meter data and found it to be about 1 cm $s^{-1}$.

The measurement uncertainty of the POGO float is $\pm 2$ cm $s^{-1}$ (Rossby et al. 1991). This is substantially less than the deep signal in this region and thus is not a problem. Since the POGO error is not systematic across a section, it has minimal impact on the transport calculations presented later. Even in the worst case scenario (i.e., if the error were systematic) the uncertainty in transport for the different layers of the DWBC and Gulf Stream (see Fig. 4) is about 1.5 Sv, which does not significantly affect our results.

The geostrophic velocities were referenced by matching the vertically averaged velocity for a given station pair to the normal component of the average of the bracketing POGO vectors (the three missing POGOs were interpolated). Figure 2a shows the resulting section of absolute geostrophic velocity for the central section. The upper-layer Gulf Stream is clearly evident, but the deep flow contains narrow bands of alternating equatorward and poleward flow. This pattern of deep flow has been seen in other absolute velocity sections near the crossover (Richardson and Knauss 1971; Joyce et al. 1986). Richardson and Knauss (1971) concluded that the Gulf Stream extended to the bottom in a narrow band, and that southward flowing jets on either side were parts of the DWBC. Their argument was based on the fact that the deep oxygen core (indicative of northern waters) extended throughout the bands of alternating flow. Our property sections show the same thing (Fig. 2b). However, the bottom current meters from the SYNOP array have indicated that this region often contains energetic topographic Rossby waves superposed on the DWBC. Using these data, Pickart and Watts (1990) have shown that the dominant waves have periods on the order of 40 days, wavelengths on the order of 100 km, and vertical trapping scales of roughly 1500 m. Thus, the bands of deep flow in Fig. 2a are most likely the signature of such waves.

In an effort to resolve the DWBC in the presence of the topographic waves, we designed a simple filtering scheme to remove the high wavenumber signal. Specifically, we smoothed each velocity section along density surfaces using a second-order Butterworth filter of width 150 km. This width was chosen because it removes 85% of the amplitude of a 100-km wave, yet retains 85% of the amplitude of a DWBC 150 km wide; such a length scale for the DWBC is implied by the tracer signal (Fig. 2b), which is not sensitive to the waves. Since we did not wish to smooth the upper-layer Gulf Stream, the filter was applied only on density surfaces deeper than $\sigma_3 = 40.45$ (Fig. 2a). To avoid a discontinuity at this depth, the filter width was ramped from 20 km to 150 km over a 300-m depth interval; the resulting velocity profiles for each station pair were then smoothed again vertically using a Gaussian filter. The final smoothed velocity section at the central line is shown in Fig. 3 along with the high-passed residual. It is clear that the filter was effective in removing the topographic wave signature and revealing the DWBC. Each of the five velocity sections was smoothed in this manner, though only one other (section 1, Fig. 1) had a significant wave signal; the other three sections remained basically unaltered (no waves were evident south of the crossover).

## 3. The shallow crossing

To study how the shallow DWBC crosses the Gulf Stream, we considered the density layer that contains the CFC core of this water mass. It turns out, however, that the top half and lower half of the water mass do very different things upon encountering the Gulf Stream. It was thus necessary to split the density layer and consider each sublayer separately (Fig. 4). Hereafter we will refer to the upper sublayer as the "upper" layer and the lower sublayer as the "intermediate" layer; remember, however, that the two layers are adjacent and together they comprise a single water mass. In this section, we consider the crossing of the upper and intermediate layers. In the next section, we consider the deep layer of Norwegian–Greenland overflow water (Fig. 4).

Figure 5 shows the lateral distribution of F-11 averaged within each sublayer. The upper layer shows a tongue getting pulled from the boundary by the Gulf Stream, with very little F-11 found at the southernmost section. The intermediate layer also has a tongue extending to the northeast, but it is located farther offshore and has a portion that extends to the southwest. In addition, part of the boundary tongue continues equatorward. The impression one gets from these lateral maps is that in the upper layer the DWBC completely recirculates with the Gulf Stream, while in the intermediate layer some of the water recirculates, but some manages to cross under the Gulf Stream (either by a direct route against the boundary or a route that takes it offshore). We must of course be careful in making inferences about the circulation from the tracer

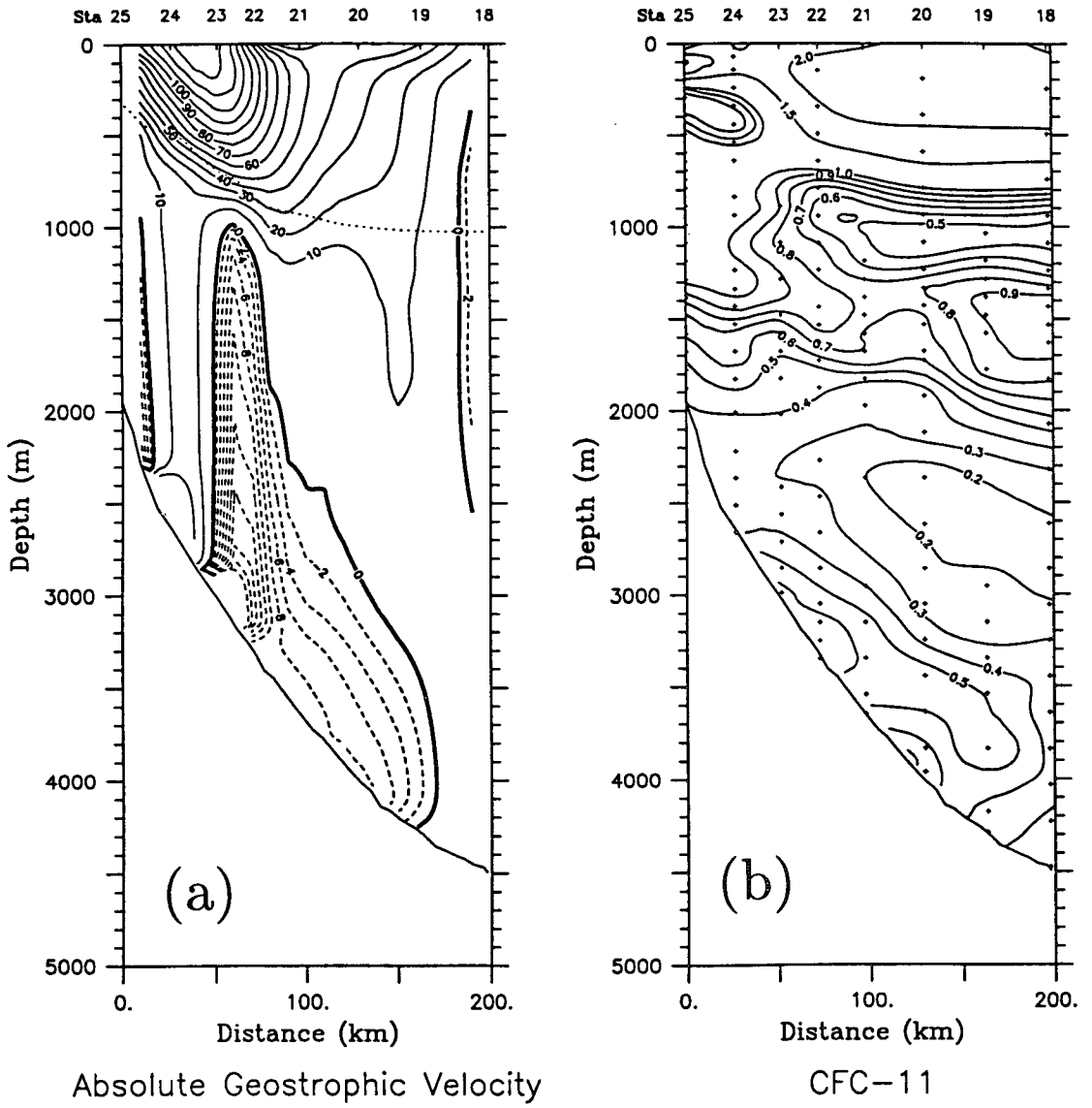


FIG. 2. (a) Absolute geostrophic velocity at section 3 (cm $s^{-1}$). Note the smaller contour interval for the equatorward flow. The dotted line is the $\sigma_3$ = 40.45 kg $m^{-3}$ density surface, below which the filter was applied (see text). (b) CFC F-11 (pM $kg^{-1}$) at section 3; the Norwegian–Greenland overflow core is the deep region greater than 0.3 pM $kg^{-1}$.

fields but, as is shown below, the velocity data are consistent with this tracer pattern.

### *a. Kinematics*

The hydrographic station plan (Fig. 1) was designed to provide high resolution of the alongstream velocity components of both the southwestward flowing DWBC and the northeastward flowing Gulf Stream. However, it is evident from the tracer tongues that protrude from the boundary (Fig. 5) that it is desirable to have the cross-stream (cross slope) component as well. For this reason we applied the dynamic method to pairs of stations from adjacent sections to get the net cross-stream component (Fig. 6a). These velocities were referenced in analogous fashion using the POGO data, and cross-stream filtered as described above. The result is a set of absolute geostrophic vectors along the four midpoint lines (the alongstream component was interpolated from the original section lines, Fig. 6b). Admittedly these vectors are "asymmetric" in that the alongstream component is closer to a point measurement while the cross-stream component is an average value (station spacing for this component averaged 170 km). However, recall that the alongstream component has been smoothed with a filter width of 150 km and, in fact, the resulting flow patterns provide meaningful information. In the surface layer the vectors clearly

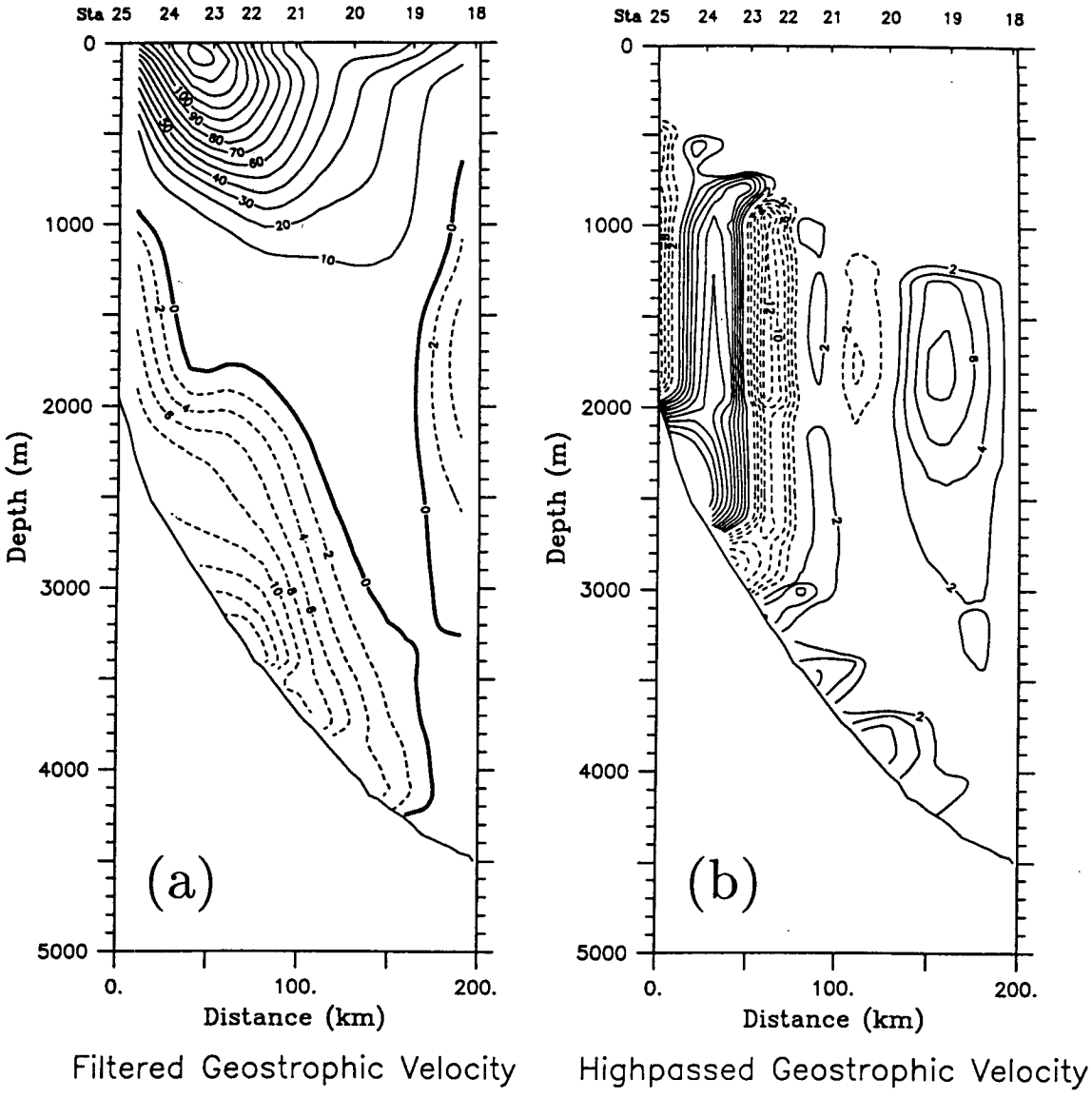


FIG. 3. (a) Low-passed geostrophic velocity at section 3. (b) High-passed signal that was removed by the filter.

reveal the separating Gulf Stream and the associated entrainment of slope water and Sargasso Sea water into the Gulf Stream (Fig. 6b).

To analyze the velocity vectors, we defined a rectangular domain oriented southwest to northeast (Fig. 6b), with $x$, $u$ positive to the northeast and $y$, $v$ positive upslope. We subjectively interpolated the vectors between midpoint lines using the original velocity sections as a guide, then applied a spline-Laplacian interpolator to put the velocities ($u$ and $v$) onto a regularly spaced grid. Trajectories were then computed by integrating from areas of inflow into the domain. The assumption here is that the smoothed velocity field is representative of the mean (recall that the waves are removed). Certainly the Gulf Stream is meandering, but the standard deviation of lateral displacements in this area is less than 10 km (Pickart and Watts 1990), which is much less than the station spacing of our survey. It is important to note that we are unable to compute an absolute dynamic height because the velocity field is in fact horizontally divergent (this should come of little surprise based on the disparity between the cross-stream and alongstream station spacing). However, the areas of significant divergence are few, and the mean divergence over the domain is less than the vorticity.

The trajectories in the upper and intermediate density layers (Fig. 7) are strikingly consistent with the corresponding tracer fields. In the upper layer all of the DWBC recirculates with the Gulf Stream. The vertical section of velocity at section 5 (not shown) in-

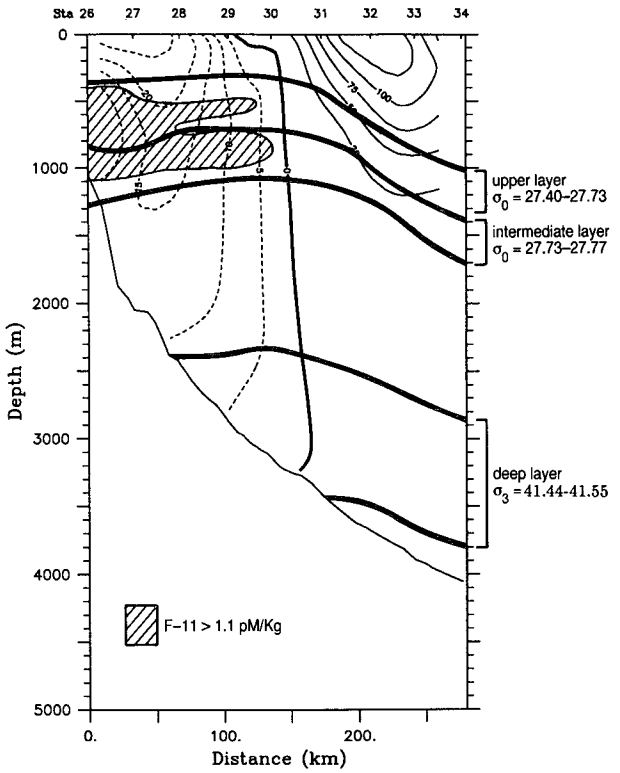


FIG. 4. Density layers of the DWBC that are analyzed in the text (thick lines), overlayed on absolute geostrophic velocity at section 2. The shaded region is the F-11 core of the shallow DWBC.

dicates that there is a strong flow of Gulf Stream water off the shelf in this density layer, hence the dashed extensions in Fig. 7a. In the intermediate layer some of the DWBC recirculates, but the onshoremost portion turns again to the southwest and continues equatorward. This "split" is precisely what is seen in the CFC distribution. It is important to note that there is no Gulf Stream water of this density on the shelf, so the dashed extensions in Fig. 7b must come from the north; the recirculated DWBC (plus offshore entrainment) forms the subsurface Gulf Stream.

It is seen then that as a result of crossing the Gulf Stream, the shallow DWBC gets sheared in half; only a portion of the intermediate layer makes it across. However, much of the DWBC transport lost to the Gulf Stream is immediately replaced by entrainment of offshore water into the DWBC on the other side of the crossover (Fig. 7). In the upper layer the DWBC transports 7.3 Sv into the crossover, and despite the complete recirculation, 4.5 Sv is flowing equatorward south of the crossover in the same layer. That this water originates from offshore is seen by its very low CFCs (Fig. 7). In the intermediate layer, 5.4 Sv approaches the crossover and 4.3 Sv exits, but in this layer the exiting water has a large CFC content (though substantial entrainment of offshore water occurs in this layer as well). It should be noted that the inflow and outflow transports in Fig. 7 are obtained by integrating the northernmost and southernmost vertical sections and are not based on the trajectories (which are only resolved in the limited rectangular domain). The outflow transport to the northeast implies that in both layers the subsurface Gulf Stream entrains a significant amount of offshore water (indicated by the dashed lines

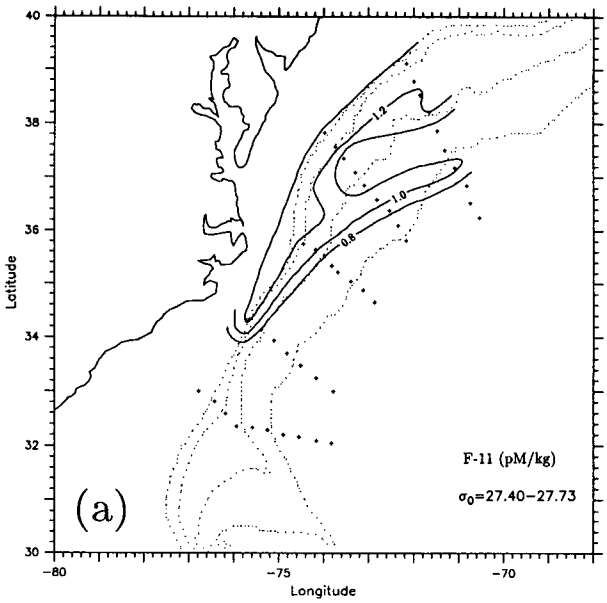


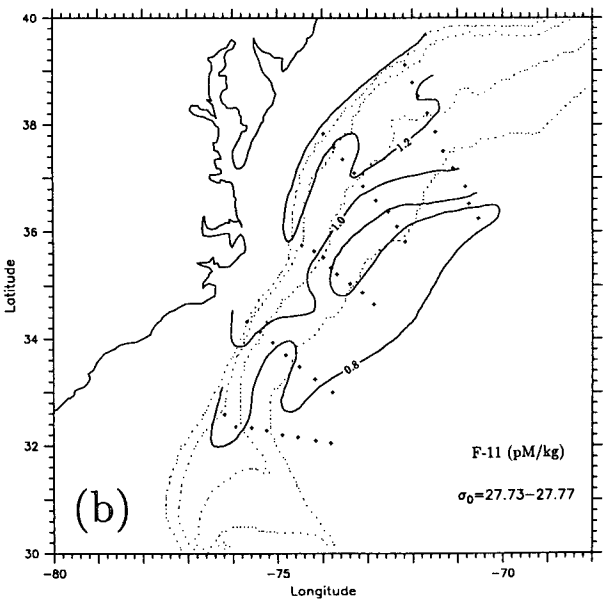


FIG. 5. Map of F-11 averaged within the indicated density layer (see Fig. 4). Data points are indicated by the plus signs. (a) The density layer $\sigma_0$ = 27.40–27.73 kg m$^{-3}$. (b) The layer $\sigma_0$ = 27.73–27.77 kg m$^{-3}$.

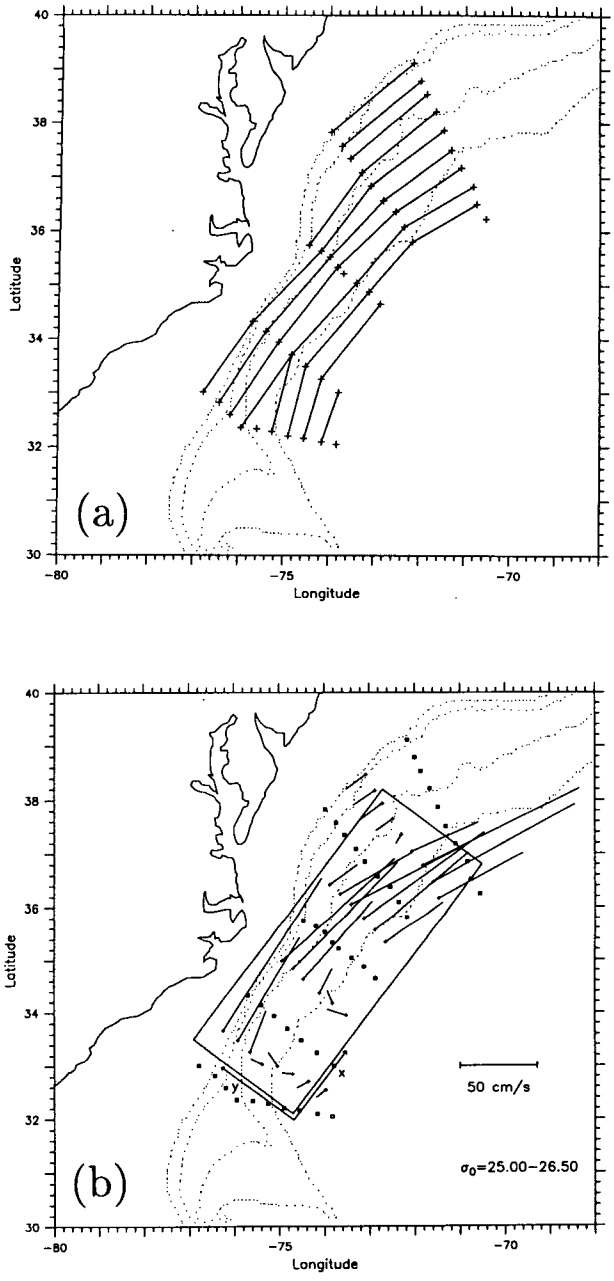


FIG. 6. (a) Station pairs used for computing the cross-slope component of velocity. (b) Absolute geostrophic velocity vectors for the surface layer ($\sigma_0$ = 25.00–26.50 kg m$^{-3}$). The original station locations are indicated by open squares. The rectangular domain is the region over which the velocities were gridded; the origin of the coordinate system is the southeast corner of the box, with $x$ positive downstream and $y$ positive upslope.

in Figs. 7a and 7b). The large CFC content of this Gulf Stream outflow implies that the offshore water being entrained has a non-negligible amount of CFCs; this is consistent with previous observations (Smethie 1993).

This recirculation and immediate replacement of the shallow DWBC at the crossover has a profound effect on the properties of the current. The CFC core (which is used as a DWBC tracer farther downstream) gets substantially deeper, denser, and saltier (remember, its

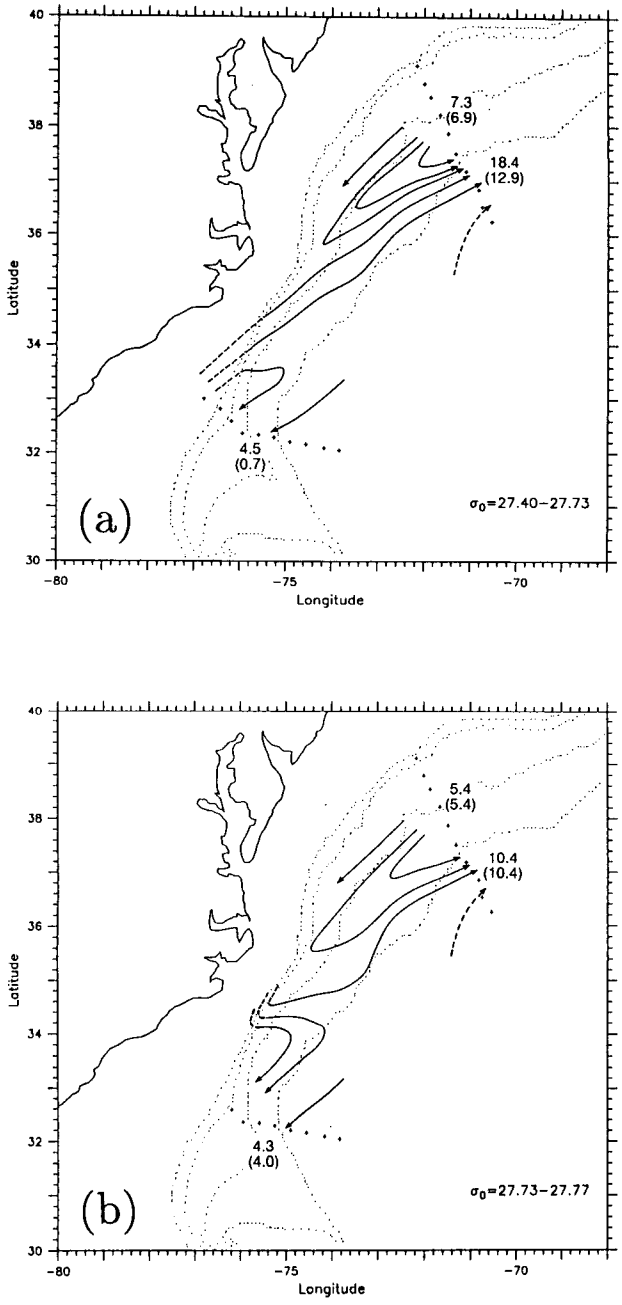


FIG. 7. Flow trajectories for the indicated density layer. The dashed portions are extrapolations outside of the rectangular domain (Fig. 6b). Indicated in bold are the inflow and outflow transports (in Sv) computed across sections 1 and 5 (plus signs). The transport of water with F-11 > 0.7 pM kg$^{-1}$ is indicated in parentheses. (a) The density layer $\sigma_0$ = 27.40–27.73 kg m$^{-3}$. (b) The layer $\sigma_0$ = 27.73–27.77 kg m$^{-3}$.

top half has been sheared off, and what remains is substantially diluted). This drastic altering of core properties (Table 1) is one of the reasons Weiss et al. (1985) chose the wrong core density in tracing this water northward to its source, and led them to misidentify it as Labrador Sea Water (see also Pickart 1992a). Note that since the recirculated DWBC transport is replaced by offshore entrainment, it is incorrect to view the DWBC as becoming denser at the crossover (only the tracer signal becomes denser). Thus, it is more meaningful to consider the change in DWBC properties averaged within the bounding density layer (i.e., the composite of the two sublayers). This was done using the CFC core to define the lateral extent of the current. As a result of the Gulf Stream crossover, the shallow DWBC becomes markedly deeper, warmer, saltier, and lower in CFCs (Table 1).

### b. *Dynamics*

The preceding kinematical description clearly involves complex dynamics, and no attempt is made here to sort everything out. However, the lateral distributions of potential vorticity do shed light on the processes involved and help clarify the dynamical distinction between the upper- and intermediate-layer crossing. We computed the potential vorticity $Q = (f + \zeta)/H$ within each layer, where $H$ is the layer thickness and $\zeta = v_x - u_y$ is the relative vorticity. The layer thickness was gridded onto the same domain as the velocities (Fig. 6b) and for consistency was smoothed in the same manner. Figure 8a shows the relative vorticity for the upper layer; the zero line separates from the boundary corresponding to the center of the Gulf Stream. Note that $\zeta$ is almost everywhere less than 5% of $f$, so that in this subsurface layer (and the deeper layers as well) the relative vorticity is nearly negligible, that is, $Q \approx f/H$ (although we still compute the full potential vorticity). Figure 8b shows the layer thickness for the upper layer, which is characterized by a tongue of small thickness corresponding to the Gulf Stream. This subsurface minimum in layer thickness is present as well in a time series of Gulf Stream Pegasus sections at 73°W (near our section 2; A. Bower 1992, personal communication).

In terms of $Q$ this feature corresponds to a ridge of high potential vorticity extending from the boundary (Fig. 9a). The fact that all of the DWBC recirculates at this depth can thus also be viewed in terms of this $Q$ barrier; to continue equatorward the water would have to pass completely through this ridge. One might envision that as the low-$Q$ DWBC water recirculates with the Gulf Stream, it stays along the inshore edge of the ridge, thus maintaining its potential vorticity. Our data indicate, however, that this is not the case. Instead, as the DWBC water becomes entrained into the Gulf Stream, its potential vorticity is increased, that is, it penetrates the ridge (Fig. 9a). Figure 9b plots $Q$ along a Gulf Stream trajectory and a DWBC trajectory. One sees that during entrainment, the DWBC trajectory is raised to the level of the Gulf Stream. Note that further downstream this level begins to drop; thus, as the Gulf Stream entrains more and more low-$Q$ DWBC water, its potential vorticity is altered (i.e., the ridge weakens).

The situation is different for the intermediate layer. As seen in Fig. 10 the downstream Gulf Stream is again characterized by a minimum in layer thickness, but upstream there is a region of nearly uniform layer thickness extending seaward from the center of the Gulf Stream. This has an important consequence; in terms of $Q$, a broad plateau upstream becomes a ridge downstream. Thus, once a DWBC trajectory penetrates the plateau, it can proceed either to the northeast or southwest and maintain its potential vorticity (Fig. 11a); that is, the $Q$ barrier for equatorward flow has been lessened. Note that this option is only available for the onshoremost DWBC trajectories. As was true in the upper layer, the level of potential vorticity decreases downstream in the Gulf Stream (Fig. 11b); however, it increases slightly progressing equatorward in the DWBC. This is consistent—the DWBC entrains a substantial amount of (higher potential vorticity) water from offshore.

It is interesting to note that in the surface layer (30–100 m) the slope water that is entrained into the Gulf

TABLE 1. Change in properties of the shallow component of the DWBC through the crossover. The left-hand entry in each column is the average value of the property within the CFC core. The core is defined as the area where F-11 $\geq$ 0.85 of the maximum value. The right-hand entry (in parentheses) is the average value of the property within the density layer $\sigma_0$ = 27.40–27.77 kg m$^{-3}$, where the lateral boundaries are determined by the CFC core.

| Section | Density $\sigma_0$ (kg m$^{-3}$) | Depth (m) | Potential temperature (°C) | Salinity (psu) | F-11 (pM kg$^{-1}$) |
|---|---|---|---|---|---|
| 1 | 27.716 | 768 (772) | 4.49 (4.76) | 34.978 (34.988) | 1.40 (1.23) |
| 2 | 27.699 | 687 (725) | 4.63 (4.78) | 34.977 (34.993) | 1.43 (1.11) |
| 3 | 27.714 | 851 (930) | 4.57 (4.77) | 34.988 (34.998) | 1.20 (1.02) |
| 4 | 27.750 | 1468 (1303) | 4.37 (5.26) | 35.004 (35.050) | 0.90 (.71) |
| 5 | 27.739 | 1263 (1179) | 4.56 (5.24) | 35.017 (35.049) | 0.92 (.72) |

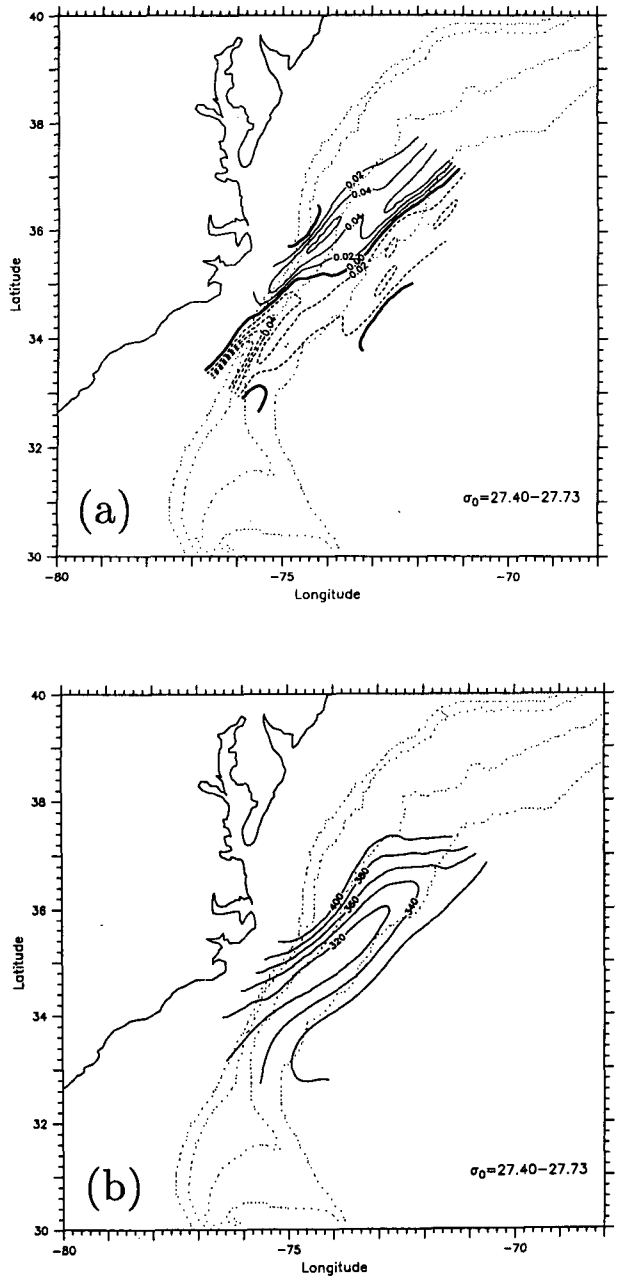


FIG. 8. (a) Relative vorticity normalized by $f$, for the density layer $\sigma_0$ = 27.40–27.73 kg m$^{-3}$. (b) Layer thickness (m) for the same density layer.

Stream does not have its potential vorticity altered (in contrast to the entrained DWBC water at depth). In the surface layer there is the more familiar front of potential vorticity across the Gulf Stream with low values offshore and high values onshore (Fig. 12a). In this case the recirculated slope water flows parallel to the front (i.e., no penetration occurs as in the deep water, Fig. 12b). Note that the transition between the Gulf Stream and slope water is marked by a maximum in potential vorticity (Fig. 12a), hence the slope water $Q$ contours turn with the trajectories.

It remains to be determined how the potential vorticity of the shallow DWBC is increased in the entrainment process. Here we offer one possibility. Recalling our assertion that the smoothed fields are representative of the mean, following a streamline the mean potential vorticity will be altered through divergence of the eddy flux of potential vorticity. In a layer approximation this statement can be written (e.g., Hogg 1983),

$$\frac{D}{Dt}\bar{Q} = -\nabla\cdot\overline{\mathbf{u}'Q'}, \tag{1}$$

where

$$\overline{\mathbf{u}'Q'} = \overline{\mathbf{u}'\zeta'} + \frac{f_0}{H\bar{T}_z}\overline{\mathbf{u}'T'}. \tag{2}$$

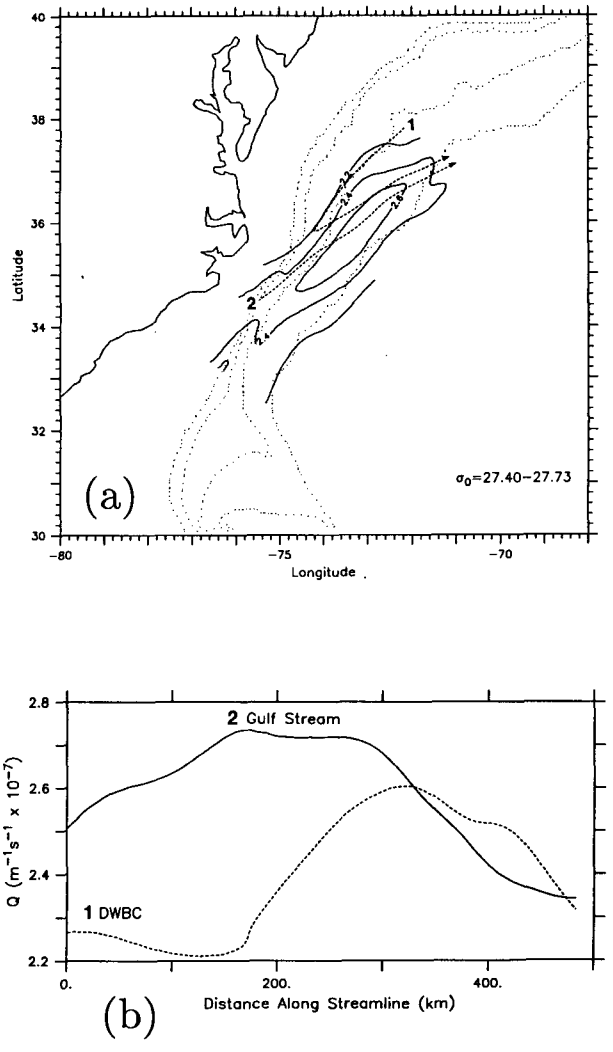


FIG. 9. (a) Potential vorticity (solid lines) in the layer $\sigma_0$ = 27.40–27.73 kg m$^{-3}$. The dashed lines are trajectories. (b) Potential vorticity plotted along the two trajectories in (a).

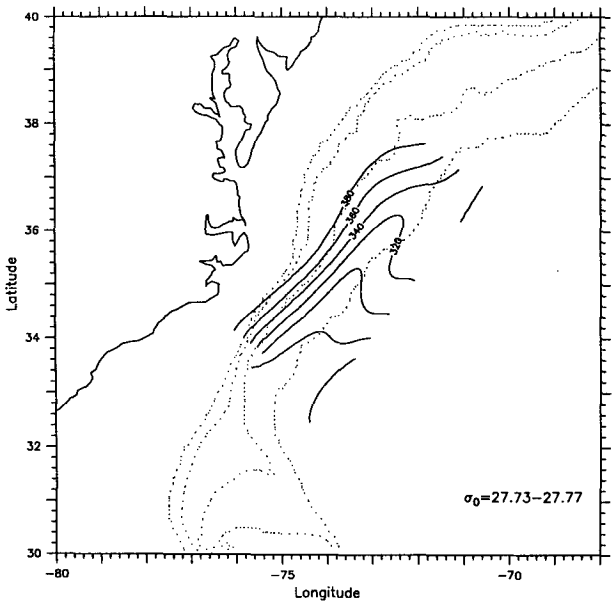


FIG. 10. Layer thickness (m) for the layer $\sigma_0$ = 27.73–27.77 kg m$^{-3}$.

The overbar denotes a time average and the primed variables are fluctuations from the mean state; $f_0$ is the (constant) Coriolis parameter, $H$ is the mean layer thickness, and $\bar{T}_z$ is the mean vertical temperature gradient (all three quantities are positive). This equation states that $\bar{Q}$ will be altered either by divergence of eddy flux of relative vorticity or divergence of eddy heat flux. A three-year time series of Pegasus temperature and velocity sections in the Gulf Stream at 73°W (near section 2, see Halkin and Rossby 1985) affords an opportunity to consider the eddy heat flux term. Since this time series consists of reoccupations of a single section, only the cross-stream component can be computed. The section of mean cross-stream eddy heat flux (Fig. 13a) shows a pronounced maximum near the Gulf Stream north wall, extending downward and southward with the main thermocline. This is plausible since the largest temperature fluctuations (due to meandering) occur in these regions. Such a distribution implies a convergence of eddy heat flux on the cyclonic side of the Gulf Stream where the entrainment occurs (Fig. 13b), consistent with an increase in $\bar{Q}$. Taking the strength of this convergence and computing $\bar{T}_z$ from the CTD data, the magnitude of the potential vorticity forcing can be estimated. We find that this forcing is more than sufficient (by roughly an order of magnitude) to raise the level of $\bar{Q}$ along a trajectory by the observed amount (Fig. 9b). Of course, the alongstream heat flux component may not be negligible (in fact, our result implies that it partially compensates), and the relative vorticity contribution may even be the dominant effect. Clearly this requires further study; we have only suggested a possible baroclinic mechanism resulting from fluctuations of the Gulf Stream.

## 4. The deep crossing

### a. Kinematics

We consider now the deep density layer that corresponds to the Norwegian–Greenland overflow component of the DWBC (Fig. 4). This is the water that Richardson (1977) measured using bottom current meters in the earlier crossover study. Hogg and Stommel (1985) considered such a deep layer in their crossover model, which showed that the DWBC moved downslope as it crossed under the Gulf Stream to avoid vertical compression. Pickart and Watts (1990) presented the first observational evidence of such down-

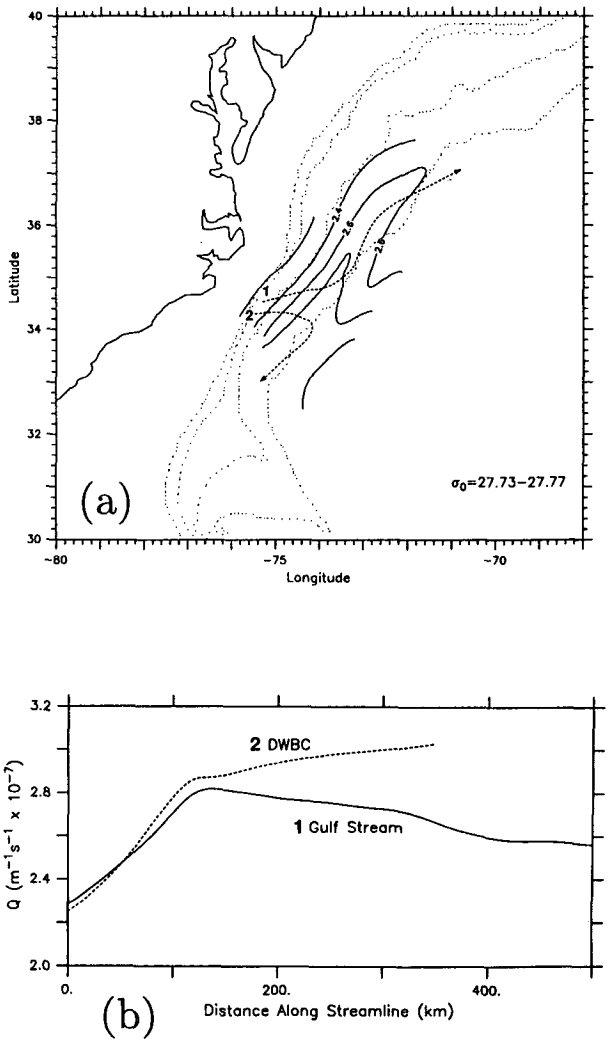


FIG. 11. (a) Potential vorticity (solid lines) in the layer $\sigma_0$ = 27.73–27.77 kg m$^{-3}$. The dashed lines are trajectories. (b) Potential vorticity plotted along the two trajectories in (a).

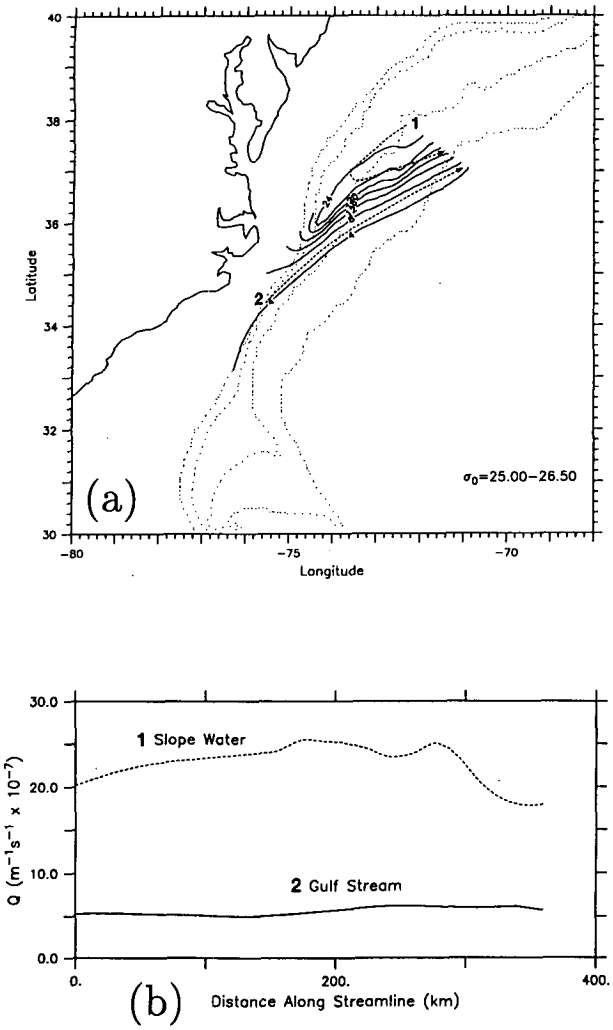


FIG. 12. Same as Fig. 11 but for the surface layer $\sigma_0$ = 25.00–26.50 kg $m^{-3}$.

slope flow using a long-term deployment of bottom current meters and inverted echo sounders.

Using the same procedures as above, we computed the flow trajectories and lateral distributions of oxygen and F-11 in the deep layer (Fig. 14). Recall that oxygen is the historical tracer of this water mass. The trajectories show a strong inflow of water from offshore, some of which recirculates to the north and is the predominant source of the deep Gulf Stream, the rest recirculating southward more than doubling the transport of this component of the DWBC. It has now been well established that the total transport of the DWBC is significantly larger south of the crossover than it is to the north (e.g., Leaman and Harris 1990; McCartney 1993). Our result (Fig. 14) suggests that part of this enhancement of transport occurs right at the crossover. The tracer fields are again strikingly consistent with the trajectories. A tongue of high oxygen and F-11 extends to the northeast with the deep Gulf Stream, and there is hint of an oxygen tongue being pulled to the southeast with flow recirculating back into the interior (such recirculation has to occur because the southward transport is greater at section 4 than at section 5). A similar feature is present in the vertical section of F-11 (section 4, not shown), but since it is not very strong it does not appear in the layer average of Fig. 14c.

In contrast to the upper layers, little of the Norwegian–Greenland overflow water recirculates with the deep Gulf Stream, which means the deep Gulf Stream oxygen/F-11 tongue is formed primarily by a diffusive effect: the recirculating water from offshore "brushes" against the DWBC and diffusively receives tracer that it then carries downstream. This is the same concept

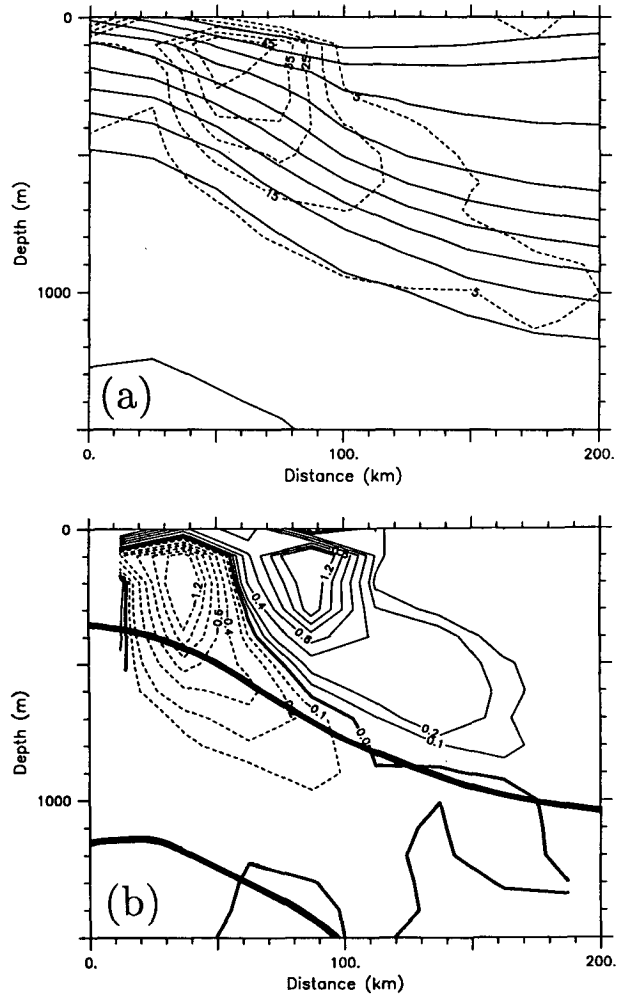


FIG. 13. (a) Vertical section of $\overline{v'T'}$ (°C cm $s^{-1}$, dashed lines) overlayed on mean temperature, calculated from a time series of Pegasus sections at 73°W (see Halkin and Rossby 1985). The temperature contours range from 4°C (deepest) to 22°C by 2°C increments. (b) Divergence of the eddy heat flux in (a) (°C cm $s^{-1}$ km). The thick lines are the bounding isotherms that correspond roughly to the density layer of the shallow DWBC (that is, the composite of the shallow and intermediate sublayers considered in the text).

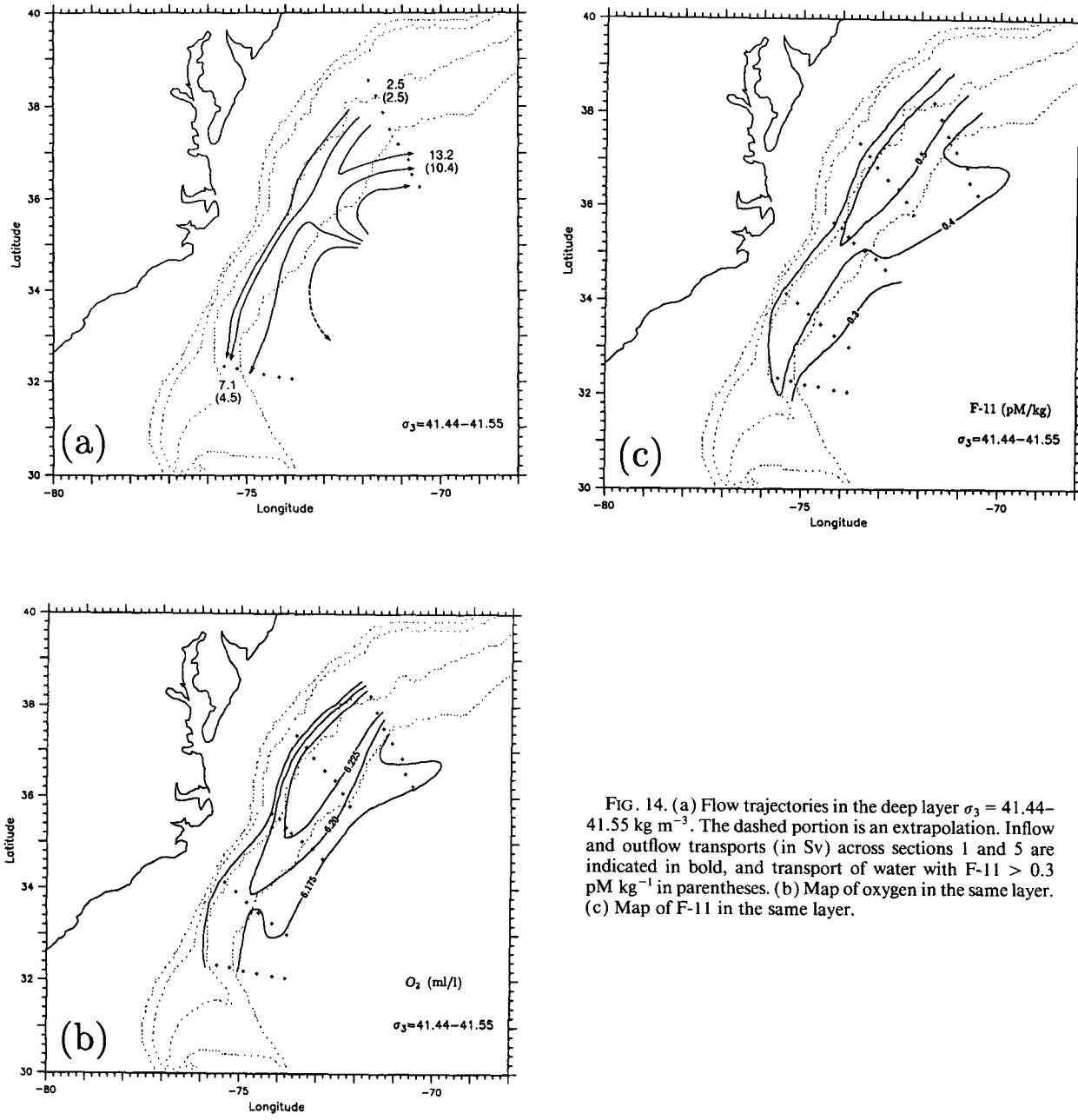


FIG. 14. (a) Flow trajectories in the deep layer $\sigma_3$ = 41.44–41.55 kg m$^{-3}$. The dashed portion is an extrapolation. Inflow and outflow transports (in Sv) across sections 1 and 5 are indicated in bold, and transport of water with F-11 > 0.3 pM kg$^{-1}$ in parentheses. (b) Map of oxygen in the same layer. (c) Map of F-11 in the same layer.

that Hogg et al. (1986) and Pickart and Hogg (1989) discussed for the deep cyclonic Gulf Stream gyre farther to the east. By contrast, most of the shallow DWBC recirculates and thus the shallow tracer tongues (Fig. 5) are primarily advective features.

Regarding changes in the properties of the DWBC resulting from the deep crossover, again there is a distinction between considering the tracer core versus the bounding density layer. Curiously, the oxygen and CFC cores become abruptly less dense and consequently shallower (Table 2) midway through the crossover (although the net change from section 1 to 5 is a deepening of the cores). We have no explanation for this; whether it is due to the crossover itself or possibly a time-dependent change propagating downstream (see Pickart 1992b) remains to be determined. In terms of the bounding density layer, the changes in the deep component of the DWBC due to the crossover are less drastic than for the shallow component. This is partly because at this depth temperature and salinity hardly

change along density surfaces extending offshore. Thus, even though the deep component of the DWBC is supplemented by offshore recirculation, it maintains its salinity and potential temperature. It does, however, become deeper and lower in oxygen/CFC content.

### *b. Dynamics*

In Hogg and Stommel's (1985) model of the deep crossover, their abyssal layer is bounded above by the main thermocline and below by the bottom topography. Observationally, our deep layer is bounded above by a deep isotherm and below by both the bottom (upslope) and a deeper isotherm (downslope; Fig. 4). This leads to an important difference regarding the layer thickness (Fig. 15); namely, the offshoremost thickness isotachs in the DWBC turn back to the northeast. This is possible because in the deep Gulf Stream the shear weakens with depth, that is, colder isotherms slope less than those above, so the layer thickness begins to decrease again offshore. Thus the deepest portion of the DWBC must recirculate in order to maintain $f/H$. The majority of the current, however, is able pass through the crossover with constant $f/H$.

These ideas are consistent with the calculated trajectories (Fig. 16a). The main body of the DWBC flows equatorward with no systematic change in potential vorticity (Fig. 16b). Also, the DWBC recirculation and the inflow from the east maintain a nearly constant $Q$. Thus, in contrast to the shallower layers, the water entrained into the abyssal Gulf Stream (and DWBC) does not have its potential vorticity altered.

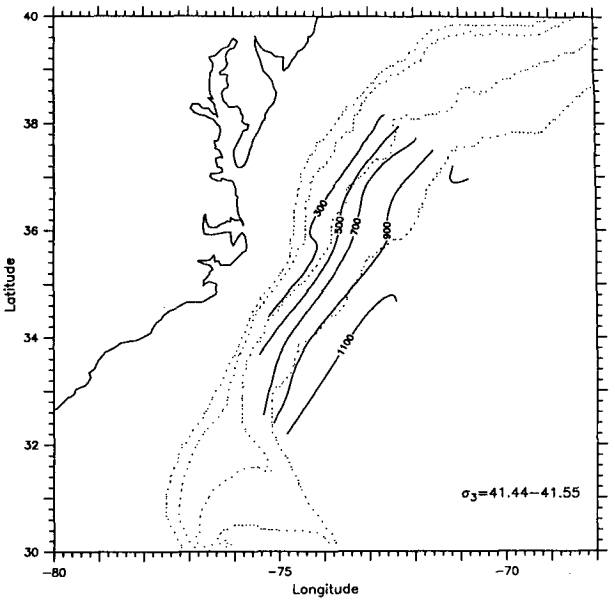


FIG. 15. Layer thickness (m) for the layer $\sigma_3$ = 41.44–41.55 kg m$^{-3}$.

## 5. Summary

A detailed hydrographic survey has provided the first clear indication of how the DWBC crosses the Gulf Stream. The passive tracer fields (CFCs and oxygen) are consistent with flow trajectories computed from the absolute geostrophic velocities. The shallow component of the DWBC (approximately 500–1200 m) is sheared in half by the Gulf Stream. Its upper sublayer collides with the strong Gulf Stream coming off the shelf and completely recirculates, transporting high CFCs into the interior. Although the lower sublayer does not encounter any flow coming off the shelf, a large portion of it recirculates, forming the subsurface Gulf Stream (together with entrainment from the Sargasso Sea). However, the onshoremost portion of the DWBC in this sublayer does progress through the crossover and continues equatorward with its high CFC signal. The recirculated DWBC transport (in both sublayers) is immediately replenished by inflow from the Sargasso Sea. Thus, there is no substantial drop in transport of the shallow DWBC, just a severe altering of its properties: most notably, the DWBC becomes markedly warmer and saltier, and its CFC content is lowered considerably.

TABLE 2. Change in properties of the deep component of the DWBC through the crossover. (a) The left-hand entry in each column of Table 2a is the average value of the property within the oxygen core. The core is defined as the area where $O_2 \geq 0.992$ of the maximum value. The right-hand entry (in parentheses) is the average value of the property within the density layer $\sigma_3$ = 41.44–41.55 kg m$^{-3}$, where the lateral boundaries are determined by the $O_2$ core. (b) The left-hand entry in each column of Table 2b is the average value of the property within the F-11 core (defined as the area where F-11 $\geq$ 0.85 of the maximum value). The right-hand entry (in parentheses) is explained in (a).

| | (a) | | | | | (b) | | | | |
|---|---|---|---|---|---|---|---|---|---|---|
| Section | Density $\sigma_3$ (kg m$^{-3}$) | Depth (m) | Potential temperature (°C) | Salinity (psu) | Oxygen (ml l$^{-1}$) | Density $\sigma_3$ (kg m$^{-3}$) | Depth (m) | Potential temperature (°C) | Salinity (psu) | F-11 (pM kg$^{-1}$) |
| 1 | 41.514 | 2914 (2854) | 2.23 (2.33) | 34.921 (34.926) | 6.28 (6.22) | 41.522 | 2987 | 2.16 | 34.918 | 0.68 (0.48) |
| 2 | 41.520 | 3032 (2814) | 2.17 (2.37) | 34.917 (34.927) | 6.28 (6.24) | 41.529 | 3120 | 2.10 | 34.913 | 0.66 (0.51) |
| 3 | 41.523 | 3355 (3035) | 2.16 (2.36) | 34.918 (34.928) | 6.25 (6.22) | 41.536 | 3280 | 2.05 | 34.913 | 0.61 (0.47) |
| 4 | 41.512 | 3240 (3101) | 2.25 (2.38) | 34.923 (34.929) | 6.20 (6.19) | 41.523 | 3250 | 2.16 | 34.918 | 0.56 (0.44) |
| 5 | 41.516 | 3289 (3145) | 2.22 (2.34) | 34.922 (34.928) | 6.21 (6.19) | 41.510 | 3113 | 2.26 | 34.923 | 0.49 (0.32) |

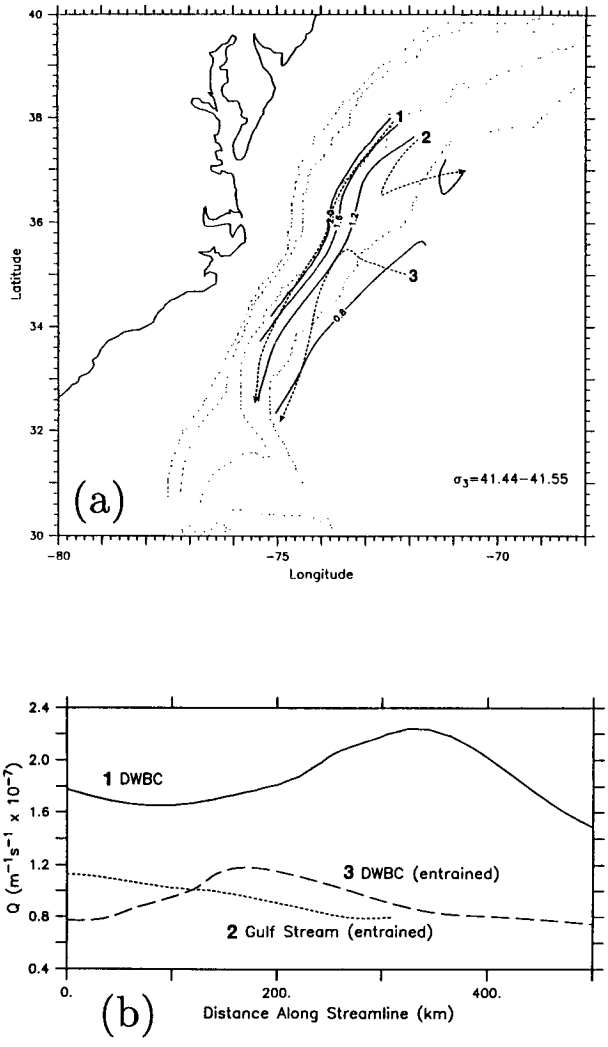


FIG. 16. (a) Potential vorticity (solid lines) in the layer $\sigma_3$ = 41.44–41.55 kg $m^{-3}$. The dashed lines are trajectories. (b) Potential vorticity plotted along the three trajectories in (a).

The potential vorticity fields for the two sublayers of the shallow DWBC help explain why these layers behave so differently at the crossover. In the upper sublayer the incoming DWBC cannot cross the ridge of high potential vorticity corresponding to the Gulf Stream, though during the subsequent entrainment the DWBC has its potential vorticity increased to the level of the Gulf Stream. Farther downstream the potential vorticity level in the Gulf Stream begins to drop, presumably by entraining so much DWBC water. Thus, the substantial recirculation at the crossover may affect the dynamics of the separated Gulf Stream by altering its potential vorticity. In the lower sublayer the presence of a plateau of potential vorticity (instead of a ridge) enables the onshoremost portion of the DWBC to progress equatorward without further change in its potential vorticity.

The deep component of the DWBC (approximately 2500–3500 m) is not as drastically altered at the crossover. Little of this component recirculates to the northeast with the Gulf Stream, though what remains is enhanced by a large inflow from the Sargasso Sea. Since the $\theta$–$S$ characteristics of this inflow are the same as the DWBC, the DWBC properties are not largely effected (aside from the sudden jump in transport). The inflow from the Sargasso Sea is also the predominant source of the deep Gulf Stream. The deep potential vorticity distribution indicates that the equatorward flowing DWBC, as well as its small recirculation with the Gulf Stream, conserves potential vorticity.

*Acknowledgments.* We are thankful to Jim Fontaine and Tom Rossby for building the POGO floats. Terry McKee quality controlled the water sample data. Tom Rossby provided the Pegasus data. This work was supported by a grant from the National Science Foundation and Office of Naval Research Grant OCE 90-09464.

## REFERENCES

Agra, C., and D. Nof, 1993: Collision and separation of boundary currents. *J. Phys. Oceanogr.*, **23,** submitted.

Barrett, J. R., Jr, 1965: Subsurface currents off Cape Hatteras. *Deep-Sea Res.*, **12,** 173–184.

Fine, R. A., and R. L. Molanari, 1988: A continuous deep western boundary current between Abaco (26.5°N) and Barbados (13°N). *Deep-Sea Res.*, **35,** 1441–1450.

Halkin, D., and T. Rossby, 1985: The structure and transport of the Gulf Stream at 73°W. *J. Phys. Oceanogr.*, **15,** 1439–1452.

Hogg, N. G., 1983: A note on the deep circulation of the western North Atlantic: Its nature and causes. *Deep-Sea Res.*, **30,** 945–961.

——, and H. Stommel, 1985: On the relationship between the deep circulation and the Gulf Stream. *Deep-Sea Res.*, **32,** 1181–1193.

——, R. S. Pickart, R. M. Hendry, and W. M. Smethie, Jr., 1986: The northern recirculation gyre of the Gulf Stream. *Deep-Sea Res.*, **33,** 1139–1165.

Johns, E., D. R. Watts, and H. T. Rossby, 1989: A test of geostrophy in the Gulf Stream. *J. Geophys. Res.*, **94,** 3211–3222.

Joyce, T. M., C. Wunsch, and S. D. Pierce, 1986: Synoptic Gulf Stream velocity profiles through simultaneous inversion of hydrographic and acoustic Doppler data. *J. Geophys. Res.*, **91,** 7573–7585.

Leaman, K. D., and J. E. Harris, 1990: On the average absolute transport of the deep western boundary currents east of Abaco Island, the Bahamas. *J. Phys. Oceanogr.*, **20,** 467–475.

McCartney, M. S., 1993: The crossing of the equator by the deep western boundary current in the western Atlantic Ocean. *J. Phys. Oceanogr.*, **23,** 1953–1974.

Olson, D. B., O. B. Brown, and S. R. Emmerson, 1983: Gulf Stream frontal statistics from Florida Straits to Cape Hatteras derived from satellite and historical data. *J. Geophys. Res.*, **88,** 4569–4577.

Pickart, R. S., 1992a: Water mass components of the North Atlantic deep western boundary current. *Deep-Sea Res.*, **39,** 1553–1572.

——, 1992b: Space–time variability of the deep western boundary current oxygen core. *J. Phys. Oceanogr.*, **22,** 1047–1061.

——, and N. G. Hogg, 1989: A tracer study of the deep Gulf Stream cyclonic recirculation. *Deep-Sea Res.*, **36,** 935–956.

——, and D. R. Watts, 1990: Deep western boundary current variability at Cape Hatteras. *J. Mar. Res.*, **48,** 765–791.

——, and S. S. Lindstrom, 1993: A comparison of techniques for referencing geostrophic velocities. *J. Atmos. Oceanic Technol.*, in press.

Richardson, P. L., 1977: On the crossover between the Gulf Stream and the western boundary undercurrent. *Deep-Sea Res.*, **24,** 139–159.

——, and J. A. Knauss, 1971: Gulf Stream and western boundary undercurrent observations at Cape Hatteras. *Deep-Sea Res.*, **18,** 1089–1109.

Rossby, T., J. Fontaine, and J. Hummon, 1991: Measuring mean velocities with POGO. *J. Atmos. Oceanic Technol.*, **8,** 713–717.

Smethie, W. M., Jr., 1993: Tracing the spreading of North Atlantic Deep Water in the western North Atlantic deep western boundary current using the chlorofluorocarbons F-11 and F-12. *Progress in Oceanography,* Pergamon.

Thompson, J. D., and W. J. Schmitz, 1989: A limited-area model of the Gulf Stream: Design, initial experiments, and model-data intercomparison. *J. Phys. Oceanogr.*, **19,** 791–814.

Weiss, R. F., J. L. Bullister, R. H. Gammon, and M. J. Warner, 1985: Atmospheric chlorofluoromethanes in the deep equatorial Atlantic. *Nature,* **314,** 608–610.